

Articles

Quantification of the Vitamin D Receptor–Coregulator Interaction[†]

Arnaud Teichert,^{‡,§} Leggy A. Arnold,^{‡,||} Steve Otieno,[⊥] Yuko Oda,[§] Indre Augustinaite,^{||} Tim R. Geistlinger,[#] Richard W. Kriwacki,[⊥] R. Kiplin Guy,^{||} and Daniel D. Bikle^{*,§}

Endocrine Unit, University of California, San Francisco, San Francisco, California 94121, Department of Chemical Biology and Therapeutics and Department of Structural Biology, St. Jude Children's Research Hospital, 162 Danny Thomas Place, Memphis, Tennessee 38105, and Amyris Biotechnologies, Emeryville, California 94608

Received October 3, 2008; Revised Manuscript Received January 13, 2009

ABSTRACT: The vitamin D receptor (VDR) regulates a diverse set of genes that control processes including bone mineral homeostasis, immune function, and hair follicle cycling. Upon binding to its natural ligand, $1\alpha,25(\text{OH})_2\text{D}_3$, the VDR undergoes a conformational change that allows the release of corepressor proteins and the binding of coactivator proteins necessary for gene transcription. We report the first comprehensive evaluation of the interaction of the VDR with a library of coregulator binding motifs in the presence of two ligands, the natural ligand $1\alpha,25(\text{OH})_2\text{D}_3$ and a synthetic, nonsecosteroidal agonist LG190178. We show that the VDR has relatively high affinity for the second and third LxxLL motifs of SRC1, SRC2, and SRC3 and second LxxLL motif of DRIP205. This pattern is distinct in comparison to other nuclear receptors. The pattern of VDR-coregulator binding affinities was very similar for the two agonists investigated, suggesting that the biologic functions of LG190178 and $1\alpha,25(\text{OH})_2\text{D}_3$ are similar. Hairless binds the VDR in the presence of ligand through a LxxLL motif (Hr-1), repressing transcription in the presence and absence of ligand. The VDR binding patterns identified in this study may be used to predict functional differences among different tissues expressing different sets of coregulators, thus facilitating the goal of developing tissue- and gene-specific vitamin D response modulators.

The vitamin D receptor (VDR),¹ which binds $1\alpha,25$ -dihydroxyvitamin D₃ ($1\alpha,25(\text{OH})_2\text{D}_3$), contains several functional domains, including a ligand-binding domain (LBD), that mediates ligand-dependent gene regulation (1). A critical step in $1\alpha,25(\text{OH})_2\text{D}_3$ action is the induction of a LBD conformational change to form activation function 2 (AF-2) (2), a hydrophobic cleft formed by three helices and a short COOH-terminal amphipathic α -helix (H12) (3), which serves as a binding surface for coactivators (4). Unliganded nuclear receptor (NR) heterodimers associate with corepressors such

as the nuclear receptor corepressor (NCoR) and the silencing mediator of retinoic acid and thyroid hormone receptor (SMRT) (5, 6) and associated histone deacetylases (7, 8). These proteins function as adaptors to convey a repressive signal to the transcriptional apparatus by maintaining a closed chromatin structure with the histone N-terminal "tails" in a charged state tightly associated with DNA (9). Ligand binding promotes the release of corepressors and the binding of coactivators, enhancing the transcription of specific genes (10). Some coactivators, such as the SRC family (11–13), recruit other coregulators with histone acetylase activity and remodel chromatin structure. Other coactivators, such as the DRIP factors (14, 15), interact with the basal transcriptional machinery. In the unliganded state, helix 12 projects away from the globular core of the LBD, while in the liganded state this helix contacts the LBD globular core domain to create an AF-2 surface through which coactivator proteins can dock (16, 17). Upon $1\alpha,25(\text{OH})_2\text{D}_3$ binding, VDR localizes at the vitamin D response elements of target genes and recruits coactivators, which recruit histone acetyltransferase to modify histone or bridge the gap between the VDR and the transcription machinery (18). Both coactivators and corepressors can interact with overlapping surfaces on the LBD (19). It has been proposed that ligand-dependent exchange between corepressors and coactivators is caused by a difference in the length of the interacting motifs that can be accommodated by the two conformations of the

[†] This work was supported by NIH Grants AR050023 (D.D.B.), AR39448 (D.D.B.), and DK58080 (R.K.G.), Cancer Center Support Grant 2P30CA021765 (L.A.A., S.O., R.W.K., and R.K.G.), the American Lebanese and Syrian Associated Charities (ALSAC), and St. Jude Children's Research Hospital (SJCRH).

* Corresponding author: tel, 415-750-2089; fax, 415-750-6929; e-mail, Daniel.bikle@ucsf.edu.

[‡] These authors contributed equally to this work.

[§] University of California, San Francisco.

^{||} Department of Chemical Biology and Therapeutics, St. Jude Children's Research Hospital.

[⊥] Department of Structural Biology, St. Jude Children's Research Hospital.

[#] Amyris Biotechnologies.

¹ Abbreviations: $1,25(\text{OH})_2\text{D}_3$, $1,25$ -dihydroxyvitamin D₃ (calcitriol); DRIP, vitamin D receptor-interacting protein; Hr, hairless; MBP, maltose binding protein; NCoR, nuclear receptor corepressor; NR box, nuclear receptor box; SMRT, silencing mediator for retinoic acid and thyroid hormone receptors; SRC, steroid receptor coactivator; TR, thyroid hormone receptor; VDR, vitamin D receptor.

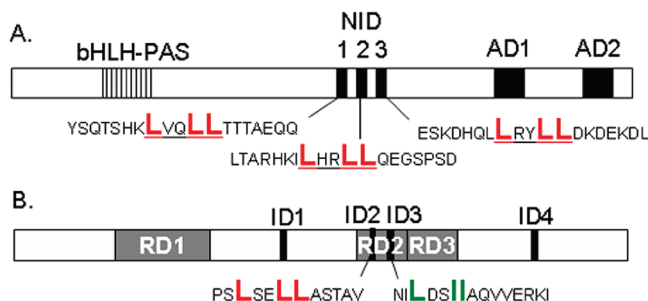


FIGURE 1: Structural composition of coregulator SRC1 and Hr. (A) Functional domains of SRC1 including the nuclear interaction domain (NID) and its three nuclear receptor interaction domains (NR boxes, SRC1-1, SRC1-2, SRC1-3). (B) Functional domains of hairless including the three transcriptional repression domains (RDs). RD2, comprised of a LxxLL and a Φ xx Φ motif, is necessary and sufficient for Hr–VDR interaction.

binding pocket (20). Therefore, a ligand that displaces the AF2 helix from its active position would be expected to facilitate the interaction with corepressor proteins and to repress transcriptional activity (21). Coactivator proteins that bind to AF-2 contain one or more of the consensus sequence LxxLL (L is leucine and x is any amino acid) which forms an amphipathic α -helix (Figure 1A) (22). This helix fits into the hydrophobic cleft of the liganded receptor (17). Receptor-specific binding of coactivators containing the LxxLL motif is governed by amino acid residues flanking the binding site, including in human VDR the conserved residues E420 and K246 (23). Mutation of these residues and adjacent hydrophobic amino acids abolishes both $1\alpha,25(\text{OH})_2\text{D}_3$ -activated transcription and coactivator interactions with the VDR (24, 25).

NR corepressors NCoR and SMRT encode multiple, short receptor interaction domains composed of the sequence Φ xx Φ (Φ is leucine or isoleucine and x is any amino acid) (26, 27). This motif is predicted to form an α -helix that is one turn longer than that formed by the LxxLL motif. In a manner analogous to the LxxLL-containing motifs, it has been suggested that this helix also binds the AF-2 surface without requiring a docked helix 12 (27). Indeed, deletion of helix 12 enhances corepressor binding (5), suggesting that this helix does not play an active role in nuclear receptor–corepressor recognition.

Another corepressor, Hr, is expressed primarily in brain, epidermis, and hair follicles (28) and is known to repress VDR-mediated transcription (29, 30). The Hr–VDR interaction is of great interest because null mutations in either protein induces alopecia in both the mouse or human (31–33). Despite a low sequence identity with other corepressors, Hr functions in a similar manner. For example, it mediates moderate transcriptional repression of liganded TR but strong repression in the case of unliganded TR (34). In contrast to TR, Hr strongly represses VDR-mediated transcription in the presence of ligand but moderately in the absence of ligand (30). Hr encodes two LxxLL motifs required for Hr–ROR α interaction (35) and two Φ xx Φ motifs required for Hr–TR interaction (Figure 1B) (30). In contrast to TR, VDR only interacts physically and functionally with Hr through a region of Hr containing a LSELL motif at position 778–782 (Hr1) and a LDSII motif at position 816–830 (Hr2) (30). As we show in this report only the LSELL motif (Hr1) mediates a ligand-dependent binding. Some VDR-mediated functions, like its control of hair follicle cycling, are ligand independent

but require Hr, suggesting a role for Hr in this VDR-regulated function (36, 37).

Ligand selectivity of VDR may affect coregulator recruitment. Published data show that VDR bound to LG190178 is able to recruit coactivator SRC2 like VDR– $1\alpha,25(\text{OH})_2\text{D}_3$ (38). Unlike $1\alpha,25(\text{OH})_2\text{D}_3$, LG190178 does not bind to serum vitamin D binding protein and exhibits no influence on calcium serum levels in mice (39). Both ligands induce HL-60 differentiation into macrophages and inhibit the growth of SK-BR-3 and LNCaP cells. Clearly, the interplay between ligand, receptor, and pools of potentially interacting coregulators is important in defining the physiological activity of VDR.

Herein we report the first comprehensive evaluation of the interaction of VDR and coregulator NR boxes using two different biochemical assays: (1) a fluorescence polarization binding assay measuring the equilibrium binding of VDR to a library of fluorescent coregulator peptides, a method that has previously been used to profile other nuclear receptor–coregulator interactions (40–42), and (2) a competition pull-down assay measuring the ability of unlabeled, but otherwise identical, coregulator peptides to inhibit the interaction between VDR and full-length SRC2. Additionally, we confirm the binding affinities of one labeled and unlabeled coregulator peptide SRC2-3 using isothermal titration calorimetry (ITC). Because of the difficulties encountered by others in working with a full-length VDR-LBD, we used a mutated form that has no major differences in ligand binding, transactivation, or dimerization with RXR α (43). The binding constants for VDR to a wide range of coregulator NR boxes including LxxLL and LxxII motifs were determined in the presence of $1\alpha,25(\text{OH})_2\text{D}_3$ and LG190178.

EXPERIMENTAL PROCEDURES

Reagents. $1\alpha,25(\text{OH})_2\text{D}_3$ (calcitriol) was purchased from Wako Chemicals USA Inc.; LG190178 was synthesized using a published procedure (39).

Protein Expression and Purification. The VDR-LBDmt, provided by D. Moras (43), was cloned by PCR (primers 5′-CGCGGATCCAGATCTGACAGTCTGCGGCCCAAG-3′ and 5′-CGCGGATCCAGATCTGACAGTCTGCGGCCCAAG-3′) at the *Bam*HI site of the pMAL-c2X vector (New England Biolabs), in fusion with the maltose binding protein (MBP). The plasmid was expressed in *Escherichia coli* grown at ambient temperature in 2× LB with 2% glucose. MBP-VDR-LBDmt protein expression was induced with 0.2 mM isopropyl 1-thio- β -D-galactopyranoside for 16 h at 25 °C before harvest and cell lysis by freeze–thawing and sonication. Proteins were purified in the absence or presence of ligand, 2 μ M ($1\alpha,25(\text{OH})_2\text{D}_3$) or 20 μ M (LG190178), using an amylose resin column.

Peptide Library Synthesis. Coregulator peptides were synthesized by the Hartwell Center (St. Jude Children’s Research Hospital), purified by RP-HPLC, and analyzed by LC/MS. The peptides containing an N-terminal cysteine were labeled using the thiol-reactive fluorophore, Texas Red maleimide (Molecular Probes): 3 mg of peptide was combined with 1.6 mg of fluorophore in 5 mL of 50% water/DMF. After being stirred for 3 h in the dark the reaction mixture was purified by HPLC and analyzed by LC/MS. All fluorescent peptides possessed purities greater than 95%.

| Peptide | -8 | -7 | -6 | -5 | -4 | -3 | -2 | -1 | 1 | 2 | 3 | 4 | 5 | 6 | 7 | 8 | 9 | 10 | 11 | 12 |
|----------|----|----|----|----|----|----|----|----|---|---|---|---|---|---|---|---|---|----|----|----|
| SRC1-1 | C | Y | S | Q | T | S | H | K | L | V | Q | L | L | T | T | T | A | E | Q | Q |
| SRC1-2 | C | L | T | A | R | H | K | I | L | H | R | L | L | Q | E | G | S | P | S | D |
| SRC1-3 | C | E | S | K | D | H | Q | L | L | R | Y | L | L | D | K | D | E | K | D | L |
| SRC2-1 | C | D | S | K | G | Q | T | K | L | L | Q | L | L | T | T | K | S | D | Q | M |
| SRC2-2 | C | L | K | E | K | H | K | I | L | H | R | L | L | Q | D | S | S | S | P | V |
| SRC2-3 | C | K | K | K | E | N | A | L | L | R | Y | L | L | D | K | D | D | T | K | D |
| SRC3-1 | C | E | S | K | G | H | K | K | L | L | Q | L | L | T | S | S | S | D | D | R |
| SRC3-2 | C | L | Q | E | K | H | R | I | L | H | K | L | L | Q | N | G | N | S | P | A |
| SRC3-3 | C | K | K | E | N | N | A | L | L | R | Y | L | L | D | R | D | D | P | S | D |
| DRIP-1 | C | K | V | S | Q | N | P | I | L | T | S | L | L | Q | I | T | G | N | G | G |
| DRIP-2 | C | N | T | K | N | H | P | M | L | M | N | L | L | K | D | N | P | A | Q | D |
| RIP140-5 | C | Q | A | A | N | N | S | L | L | L | H | L | L | K | S | Q | T | I | P | K |
| p300 | C | A | A | S | K | H | K | Q | L | S | E | L | L | R | S | G | S | S | P | N |
| NCoR-2 | C | D | P | A | S | N | L | G | L | E | D | I | I | R | K | A | L | M | G | S |
| SMRT-2 | C | H | A | S | T | N | M | G | L | E | A | I | I | R | K | A | L | M | G | K |
| Hr-1 | | | | | | C | P | S | L | S | E | L | L | A | S | T | A | V | K | L |
| Hr-2 | | | | | | C | N | I | L | D | S | I | I | A | Q | V | V | E | R | K |

FIGURE 2: Amino acid sequence of coregulator peptides. Sequence alignment of the coregulator peptides with the N-terminal cysteine label indicated in yellow, the NR box motif LxxLL in red, and the Φ xx Φ corepressor motif in green. Note: cysteine–serine exchange was employed in the case of SRC3-1 (7) and Hr1 (2) to prevent double labeling.

Peptide Binding Assay. MBP-VDR-LBDmt protein binding affinities, in the presence of $1\alpha,25(\text{OH})_2\text{D}_3$ ($2\ \mu\text{M}$) or LG190178 ($20\ \mu\text{M}$) using fluorescently labeled coregulator peptides, were measured using a previously described assay (40). The relative doses of $1\alpha,25(\text{OH})_2\text{D}_3$ and LG190178 have been described previously (39). Two different protein batches were used for two independent experiments, with each carried out in triplet. Reported values reflect the mean value with associated total error across all experiments.

Competitive Binding Assay. Fluorescently labeled SRC2 was produced by *in vitro* transcription–translation (TNT kit and FluoroTect; Promega) from the plasmid pSGT-SRC2. In a 96-well polypropylene plate (Costar 3365) eight peptides at a time were diluted from 10000 to $1.0\ \mu\text{M}$ in DMSO. Two microliters of the diluted peptides was added to $91\ \mu\text{L}$ of buffer (25 mM HEPES, 100 mM NaCl, 1 mM DTT, 0.01% NP40, 0.1% BSA (added fresh), $0.5\ \mu\text{M}$ VDRmt on amylose beads, and $1\ \mu\text{M}$ $1\alpha,25$ -dihydroxyvitamin D_3) in a 96-well filter plate (Millipore; Multiscreen HTS BV). After agitation for 2 h (IKA microtiter plate shaker) at room temperature, $7\ \mu\text{L}$ of TNT solution was added to each reaction followed by 2 h of agitation at room temperature. The filter plate was attached to 96-well plate (Costar 3365) and centrifuged at $50g$ for 3 min followed by the addition of $100\ \mu\text{L}$ of buffer (25 mM HEPES, 100 mM NaCl, 1 mM DTT, 0.01% NP40, 0.1% BSA (added fresh)). The filter plate was assembled with another 96-well plate (Costar 3365) and centrifuged at $50g$ for 3 min. For elution of the SRC2–VDR complex $10\ \mu\text{L}$ of a 10 mM maltose solution was added. After a 10 min incubation period the filter plate was assembled with another 96-well plate (Costar 3365) and centrifuged at $50g$ for 3 min. The elutions were treated with $3\ \mu\text{L}$ of $4\times$ SDS–PAGE loading buffer (Invitrogen), sealed, and incubated for 30 min in an oven at $70\ ^\circ\text{C}$. After separation using SDS–PAGE the fluorescent bands of SRC2 were visualized using a fluorescence scanner (Typhoon; GE). The bands were integrated using ImageQuant (Molecular Dynamics) and analyzed using Prism (GraphPad). Three independent experiments were carried out for each state. The IC_{50} values were obtained by fitting data to the equation $y = \min + (\max - \min) / (1 + (x/K_d))$ Hill slope.

Calorimetric Studies. The thermodynamics of the interaction between the SRC2-3 peptides and VDR-LBD were

determined using a VP-ITC instrument (Microcal, Northampton, MA). Therefore, a solution of either unlabeled or Texas Red labeled SRC2-3 peptide ($0.42\ \mu\text{M}$) in the syringe was titrated into a solution of VDR ($25\ \mu\text{M}$) in the cell. Two microliters of the titrant was first injected followed by 25 injections of $10\ \mu\text{L}$ each, with a 300 s delay between injections. The experiments were performed at $25\ ^\circ\text{C}$ in a buffer containing 20 mM HEPES, pH 7.5, and 150 mM NaCl. The binding data were fit to a 1:1 binding model using Origin software (Origin Laboratory, Northampton, MA).

RESULTS

Coregulator Peptide Library. To evaluate VDR coregulator recruitment, the binding between the VDR-LBD and a library of known coregulator peptides consisting of a central LxxLL or Φ xx Φ sequence plus up to eight additional flanking residues at each terminus was measured (Figure 2). To allow attachment of the fluorescent label, a non-native cysteine was introduced at the N-terminus of each peptide. Additionally, a cysteine–serine exchange was employed in the case of SRC3-1 and Hr1 to prevent double labeling. Hr1 contains a second cysteine residue at the -3 position of the LxxLL motif which was used for labeling. All peptide probes were synthesized in parallel using Fmoc (9-fluorenylmethyl-oxycarbonyl) protective group and purified by RP-HPLC. Identity and purity were confirmed using HPLC and MALDI-TOF or LCMS and were greater than 95%.

Initial Validation of Coactivator Peptide Binding Assay. Initial peptide binding studies were carried out with SRC2-2 in the presence of $1\alpha,25(\text{OH})_2\text{D}_3$ with both MBP-VDR-LBDwt and MBP-VDR-LBDmt, from the construct developed by D. Moras (43). Control experiments using a MBP protein alone showed no interaction with SRC2-2 (data not shown). SRC2-2 binds to both MBP-VDR-LBDwt and MBP-VDR-LBDmt in a similar saturable dose-dependent manner, with somewhat higher affinity for MBP-VDR-LBDmt observed than for MBP-VDR-LBDwt (Supporting Information). We used MBP-VDR-LBDmt for further studies because it was soluble at higher concentrations, which was essential to determine the binding constants (K_d) using fluorescence polarization. To exclude potential perturbing interactions between the label attached to the peptide and MBP-VDR-

Table 1: Isothermal Titration Calorimetry Using VDR-LBD and Coregulator Peptide SRC2-3 or SRC2-3 Labeled with Texas Red

| interaction | K_d (nM) | n | ΔH (kcal/mol) |
|----------------------|--------------|-----------------|-----------------------|
| VDR-SRC2-3 | 174 ± 37 | 1.02 ± 0.02 | -6.7 ± 0.3 |
| VDR-SRC2-3 Texas Red | 285 ± 18 | 0.93 ± 0.04 | -2.2 ± 0.12 |

LBDmt, we measured the binding affinity K_d values for labeled and unlabeled coregulator peptide SRC2-3 using isothermal titration calorimetry (ITC) (Table 1 and Supporting Information). The K_d values observed for the Texas Red labeled and unlabeled peptide SRC2-3 were 285 and 174 nM, respectively. To demonstrate the ability of unlabeled peptides to inhibit the interaction between VDR-LBD and full-length SRC2 exhibiting three LxxLL motifs, we performed pull-down competition assays. In these assays the native peptides (LxxLL) blocked this interaction, whereas altered peptides (LxxAA) did not affect this binding (Figure 3D). To verify that binding of Hr-1 is not compromised by cysteine-serine (C/S) exchange, a competitive fluorescence polarization experiment was carried out showing that Hr-1wt and Hr-1C/S equally inhibited the binding between SRC2-3 Texas Red and MBP-VDR-LBDmt (Supporting Information).

Coactivator Binding Assays. The fluorescence polarization assay was executed by maintaining a constant concentration of fluorescently labeled coactivator peptide (10 nM) and a variable concentration of VDR-LBDmt from 0.002 to 199 μ M in the absence and presence of $1\alpha,25(\text{OH})_2\text{D}_3$ or LG190178. The data were fit to a sigmoidal dose-response curve, and K_d values with 95% confidence intervals are

summarized in Figure 4. The competition pull-down assay was carried out with labeled SRC2, solid-supported VDR-LBDmt, and unlabeled coregulator peptides. Displaced fluorescent SRC2 was removed by washes, and residual SRC2 was quantified after separation by SDS-PAGE (Figure 3D). The data were fit to a sigmoidal dose-response curve, and K_d values with 95% confidence intervals are summarized in Figure 4 and Supporting Information.

Coregulator Peptides Bind VDR-LBDmt in the Absence or Presence of Ligand in Three Different Modes. Binding isotherms for coregulator peptides exhibited three behaviors: saturable binding with a clear high dosage plateau, clear interaction without saturation, and no interaction. The higher affinity group of peptides bound in a ligand-dependent, dose-dependent, and saturable manner where a plateau was reached within the protein concentration range studied (Figure 3A, ■). The K_d values for this class in the presence of ligand were lower than 20 μ M as determined by fitting the data to a sigmoidal dose-response curve. Nine coactivator peptides exhibited this mode: SRC1-2, SRC1-3, SRC2-2, SRC2-3, SRC3-2, SRC3-3, DRIP205-2, RIP140-5, and Hr1 (Figure 4, green and dark green color code). The binding affinities of these peptides in the absence of ligand were dose dependent but exhibited no plateaus at higher protein concentrations (Figure 3A, ▲). Because of the missing isotherm saturation we labeled these interactions as weak or no binding (Figure 4, gray color code, and Supporting Information). The IC_{50} values determined by an independent competition pull-down assay were similar to K_d values in the presence of ligand measured by FP.

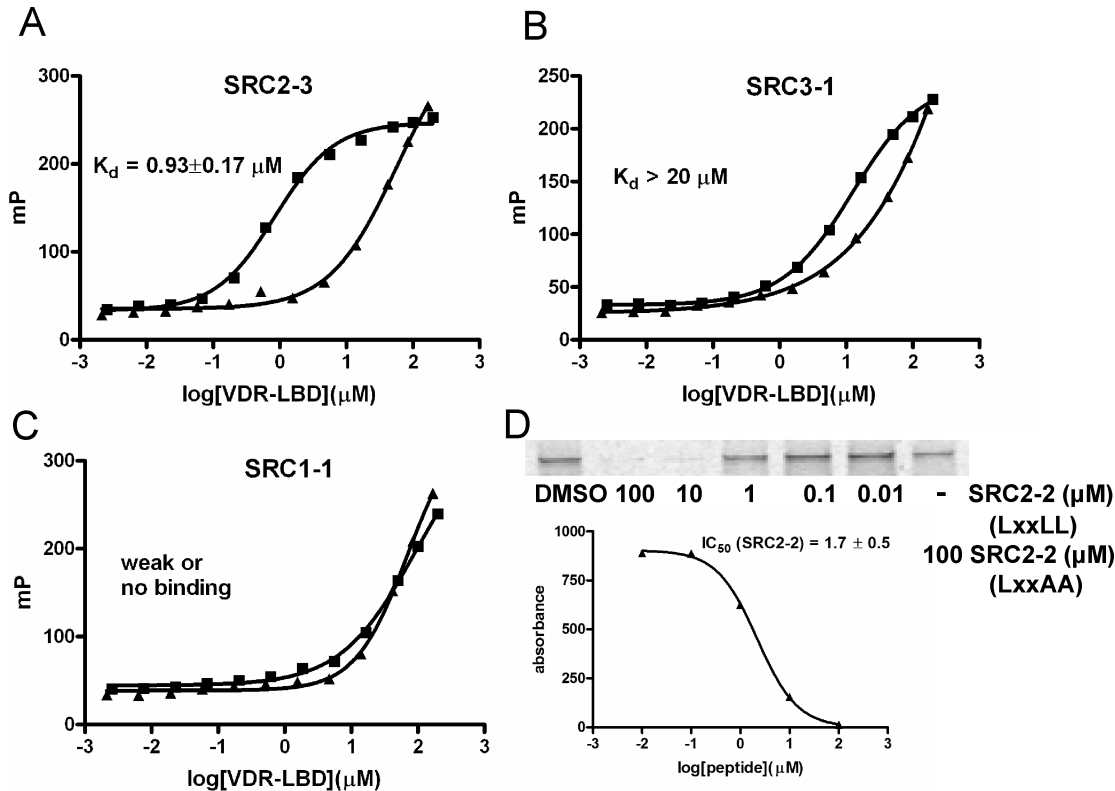


FIGURE 3: VDR-coactivator binding isotherms in the presence and absence of $1\alpha,25(\text{OH})_2\text{D}_3$: (■) $1\alpha,25(\text{OH})_2\text{D}_3$; (▲) no ligand. (A) High-affinity binding between VDR and SRC2-3 in the presence and absence of $1\alpha,25(\text{OH})_2\text{D}_3$. (B) Low-affinity binding between SRC3-1 and VDR in the presence and absence of $1\alpha,25(\text{OH})_2\text{D}_3$. (C) Weak or no binding between SRC1-1 and VDR in the presence and absence of $1\alpha,25(\text{OH})_2\text{D}_3$. (D) SRC2 full-length binding to VDR-LBD is blocked by increasing concentration of SRC2-2 peptide (LxxLL) but not by the mutated SRC2-2 peptide (LxxAA). Quantified SDS-PAGE converted into the binding isotherm to determine the IC_{50} value of SRC2-2.

| | | FP assay | | | Pull down |
|-----------|----------|--------------------------------|-----------------|-----------|--------------------------------|
| | | 1 α ,25(OH) $_2$ D $_3$ | LG190178 | No ligand | 1 α ,25(OH) $_2$ D $_3$ |
| SRC1 | SRC1-1 | | | | |
| | SRC1-2 | 1.8 \pm 0.3 | 1.1 \pm 0.2 | | 2.7 \pm 1.8 |
| | SRC1-3 | 1.4 \pm 0.1 | 1.1 \pm 0.1 | | 1.3 \pm 0.7 |
| SRC2 | SRC2-1 | | | | |
| | SRC2-2 | 1.7 \pm 0.2 | 1.7 \pm 0.3 | | 1.7 \pm 0.5 |
| | SRC2-3 | 0.93 \pm 0.17 | 0.84 \pm 0.11 | | 0.71 \pm 0.36 |
| SRC3 | SRC3-1 | | | | |
| | SRC3-2 | 7.7 \pm 2.1 | 7.1 \pm 1.8 | | 11 \pm 3 |
| | SRC3-3 | 0.97 \pm 0.12 | 0.86 \pm 0.11 | | 0.91 \pm 0.48 |
| DRIP 205 | DRIP-1 | | | | |
| | DRIP-2 | 1.6 \pm 0.2 | 1.6 \pm 0.1 | | 2.1 \pm 0.9 |
| | P300 | | | | |
| | RIP140-5 | 5.0 \pm 1.8 | 5.2 \pm 1.4 | | 6.1 \pm 2.6 |
| | NCoR | | | | |
| | SMRT | | | | |
| Hair less | Hr1 | 5.9 \pm 0.9 | 7.7 \pm 0.9 | | 6.9 \pm 2.8 |
| | Hr2 | | | | |

Equilibrium
K $_d$ (μ M)

<3

3.1–20.0

>20

Weak or
no
binding

FIGURE 4: Coregulator binding patterns and specificity determinants. The equilibrium binding constants (K_d values) for the binding of VDR to coregulator peptides (SRC1, SRC2, SRC3, DRIP205, P300, RIP140-5, NCoR, SMRT, and Hr) in the presence and absence of 1 α ,25(OH) $_2$ D $_3$ or LG190178 were determined by fluorescent polarization. IC $_{50}$ values of peptides determined by a competition pull-down assay employing VDR-LBD and full-length SRC2 in the presence of 1 α ,25(OH) $_2$ D $_3$. The K_d and IC $_{50}$ values are color coded: dark green (<3 μ M), green (3.1–20.0 μ M), light green (>20 μ M), and gray (>50 μ M, weak or no binding).

The lower affinity group included peptides exhibiting dose-dependent binding in the presence of ligand but did not display a plateau at the highest protein concentrations used. In comparison with the binding isotherm in the absence of ligand we observed a clear shift indicating ligand-dependent binding (Figure 3B). For this group of peptides we suggest a K_d value higher than 20 μ M, and the group includes SRC3-1, DRIP-1, and P300 (Figure 4, light green color code). The binding constants in the absence of ligand exhibited high values indicative of very weak binding (Figure 4, gray color code, and Supporting Information). Inhibition of binding between SRC2 and VDR was observed at concentrations of these peptides greater than 50 μ M.

The third group of peptides showed identical dose-dependent binding in the presence and absence of ligand and did not display saturation at higher concentrations of peptide. This group included SRC1-1 and SRC2-1 bearing an LxxLL motif and corepressor peptides NCoR, SMRT, and Hr2 with LxxIxxxL/V motifs (Figure 3C). The mode of binding of these peptides was indicated as weak binding or no binding (Figure 4, gray color code, and Supporting Information).

DISCUSSION

In this study, we examined the binding of VDR-LBD to a range of target motifs within potential VDR coregulators. Because of the difficulties encountered by others in working with wild-type VDR-LBD, we used a mutated form, which lacks a domain with no apparent function and little homology

to other NRs (43–46). Native VDR-LBD and VDR-LBDmt have been shown to function similarly with respect to ligand binding, transactivation, or dimerization with RXR α LBD (43). We confirmed these results by showing that SRC2-2 bound to VDR-LBDmt with high affinity in a ligand-dependent manner. We observed that VDR-LBDmt exhibited higher affinity for SRC2-2 than did native VDR-LBD, possibly due to the higher solubility of the former construct under our assay conditions.

Our results verify that VDR binds LxxLL motifs from numerous coactivators in a selective fashion. The K_d values measured for the absolute binding of coregulator motifs to the VDR are similar to those observed for binding to other nuclear receptors (40, 47). In contrast to the estrogen receptor and thyroid receptor, which have the highest affinity for the second NR box of each SRC, VDR binds to the second and third NR box with higher affinities than to the first NR box. Considering all NR boxes of each SRC, we observed the same affinity between VDR/SRC1 and VDR/SRC2. In contrast, SRC3 exhibited a stronger interaction between SRC3-1 and VDR in comparison with SRC1-1 and SRC2-1, whereas SRC3-2 has a weaker interaction with VDR in comparison with SRC1-2 and SRC2-2. This may suggest that SRC3 dominates binding to VDR relative to SRC1 or SRC2. SRC3 has been previously described as a more “general” coactivator, but our results may reveal selectivity for VDR for this protein (48).

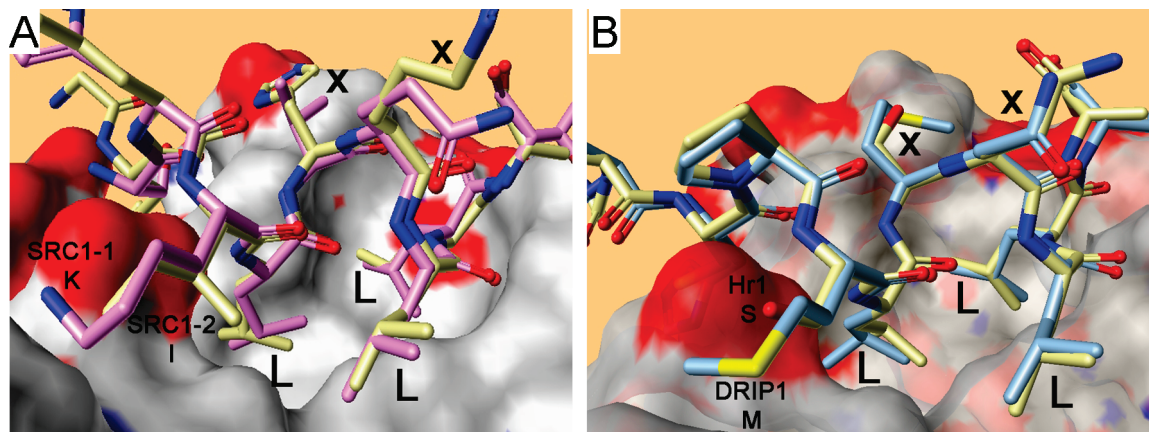


FIGURE 5: VDR-coactivator interaction. (A) Crystal structure of VDR-SRC1-2 (57) and docked SRC1-1; -1 N-terminal residue of LxxLL is K (SRC1-1) and I (SRC1-2). (B) Crystal structure of VDR-DRIP2 (53) and docked Hr1; -1 N-terminal residue of LxxLL is M (DRIP2) and S (Hr1).

It has been reported that amino acid residues N-terminal to the LxxLL motif have a major impact on the binding affinities of coregulator peptides (22, 49, 50). In particular, coregulator peptides bearing hydrophobic amino acids at the -1 position of the LxxLL motif exhibited high affinities for ER, PPAR, TR, and VDR (22, 40, 51, 52). In the case of the peptides investigated in this study we observed the same correlation. In contrast, we showed that coregulator peptides missing a hydrophobic amino acid residue at the -1 position like SRC1-1, SRC2-1, SRC3-1, P300, NCoR, and SMRT exhibited a low binding affinity toward VDR with the exception of Hr1. The crystal structure of SRC1-2 bound to VDR-LBD illustrates the importance of the isoleucine residue in contact with the hydrophobic surface of AF-2 (Figure 5A) (53). In overlay, the SRC1-1 structure exhibits a protonated lysine residue destabilizing the interaction between coregulator and VDR. Zella et al. (52) reported that VDR agonist derived LxxLL peptides, originated from a phage display screening, have the proposed sequence LxH/HxH/FPL/M/I. Because of the sequence similarity with DRIP peptides we observed a binding constant of 1.6 μ M (Figure 4) for DRIP-2 following the proposed paradigm of a HPMLxxLL sequence. In contrast DRIP-1, bearing a NPILxxLL sequence, has a weak interaction with VDR. DRIP205 is known to interact directly with ligand-activated VDR/RXR heterodimers mostly through the second motif, although both motifs are equally required for VDR-mediated transcription in cells (54).

Hr1 is part of the coregulator hairless which represses VDR-mediated transcription in the presence and absence of $1\alpha,25(\text{OH})_2\text{D}_3$ (30). Hairless interacts with VDR predominantly through the 750–864 domain, exhibiting a coactivator LxxLL motif (Hr1) and a corepressor LxxIxxxV motif (Hr2) (Figure 1B). Our investigation of these motifs separately showed that Hr2 exhibits a weak affinity toward VDR in the presence and absence of ligand in contrast to Hr1 which exhibited a $1\alpha,25(\text{OH})_2\text{D}_3$ -dependent VDR-LBD binding of 5.9 μ M (Figure 4). Because Hr1 is bearing a serine residue at the -1 N-terminal position of LxxLL (Figure 5B), this is the first reported coregulator peptide binding to VDR and bearing a polar residue at this particular position. Peptides with a similar sequence to Hr1 were identified by Zella et al. (52) in the presence of the VDR antagonist ZK15922, but binding of these peptides could not be confirmed by a two-hybrid assay (52). The binding affinities for Hr1

measured in the presence of agonist $1\alpha,25(\text{OH})_2\text{D}_3$ and LG190178 were similar for VDR. We can conclude that Hr1 is supporting the interaction between VDR and Hr in the presence of ligand. This was a surprise. Our previous findings in keratinocytes with full-length molecules showed that VDR and hairless bind to each other in the absence of ligand and that this binding is partially displaced by addition of $1\alpha,25(\text{OH})_2\text{D}_3$ (29). This suggests that results at least for hairless obtained with peptides recapitulate only partially the binding properties of full-length proteins.

Like Hr2, corepressor SMRT and NCoR peptides exhibited weak interactions with VDR in the presence and absence of ligand, although stronger interactions have been reported for full-length proteins (55, 56). The length of a polypeptide has a strong influence on its three-dimensional structure which determines binding affinity and solubility. Lower affinities of small peptide mimics in comparison with full-length proteins are not uncommon. The nature of the FP assay does not allow reliable K_d measurements of lower affinity probes due to light scattering caused by protein aggregation at high concentrations. In contrast, high-affinity probes exhibiting a saturated signal at higher protein concentrations do not suffer from this interference. Moreover, a recent study showed that NCoR- and SMRT-dependent repression of $1\alpha,25(\text{OH})_2\text{D}_3$ -mediated transcription by VDR/RXR heterodimer is achieved through their recruitment by RXR but not by VDR (56), suggesting that further studies involving VDR/RXR heterodimers are needed to determine the affinity of these corepressors for these nuclear receptors.

In the presence of synthetic agonist LG190178, VDR adopts an agonistic conformation, recruiting all investigated coregulators with the same affinities as VDR/ $1\alpha,25(\text{OH})_2\text{D}_3$. This result is supported by the fact that, in the case of VDR, crystal structures with different vitamin D_3 analogues in the presence of coregulator peptide exhibit an unaltered AF-2 domain (23, 53, 57, 58). We can conclude that the signal transduction mediated by VDR is similar regardless of which of the two ligands is bound.

The IC_{50} values determined by a competition pull-down assay confirmed the K_d values determined by the FP measurements. We reported a similar behavior for TR (59), suggesting that although full-length SRC2 exhibits multiple NR boxes, no assisted binding among them occurs in this biochemical assay.

Presumably there are additional factors that influence NR recruitment of coregulators such as posttranslational modifications, structural determinants arising from specific DNA response elements, cooperativity, cellular environment, and additional interaction surfaces on the NR and coregulator proteins, needing more complex models to fully dissect NR–coregulator interactions. These binding patterns draw a first picture of potential functional differences for different ligands in tissues with different sets of coregulators. The use of more ligands should allow us to predict these functional differences, thus facilitating the goal of developing tissue- and gene-specific vitamin D response modulators.

ACKNOWLEDGMENT

We thank Dr. Patrick Rodrigues and Bob Cassell for peptide synthesis at the Hartwell Center of Bioinformatics and Biotechnology, St. Jude Children's Research Hospital, Memphis, TN.

SUPPORTING INFORMATION AVAILABLE

FP isotherms for each Texas Red labeled peptide in the presence and absence $1\alpha,25(\text{OH})_2\text{D}_3$ and ITC isotherms of unlabeled and Texas Red labeled SRC2-3 peptide. This material is available free of charge via the Internet at <http://pubs.acs.org>.

REFERENCES

- Carlberg, C., and Polly, P. (1998) Gene regulation by vitamin D3. *Crit. Rev. Eukaryot. Gene Expression* 8, 19–42.
- Moras, D., and Gronemeyer, H. (1998) The nuclear receptor ligand-binding domain: structure and function. *Curr. Opin. Cell Biol.* 10, 384–391.
- Danielian, P., White, R., Lees, J., and Parker, M. (1992) Identification of a conserved region required for hormone dependent transcriptional activation by steroid hormone receptors. *EMBO J.* 11, 1025–1033.
- Feng, W., Ribeiro, R., Wagner, R., Nguyen, H., Apriletti, J., Fletterick, R., Baxter, J., Kushner, P., and West, B. (1998) Hormone-dependent coactivator binding to a hydrophobic cleft on nuclear receptors. *Science* 280, 1747–1749.
- Chen, J. D., and Evans, R. M. (1995) A transcriptional co-repressor that interacts with nuclear hormone receptors. *Nature* 377, 454–457.
- Kurokawa, R., Soderstrom, M., Horlein, A., Halachmi, S., Brown, M., Rosenfeld, M., and Glass, C. (1995) Polarity-specific activities of retinoic acid receptors determined by a co-repressor. *Nature* 377, 451–454.
- Heinzel, T., Lavinsky, R. M., Mullen, T. M., Soderstrom, M., Laherty, C. D., Torchia, J., Yang, W. M., Brard, G., Ngo, S. D., Davie, J. R., Seto, E., Eisenman, R. N., Rose, D. W., Glass, C. K., and Rosenfeld, M. G. (1997) A complex containing N-CoR, mSin3 and histone deacetylase mediates transcriptional repression. *Nature* 387, 43–48.
- Nagy, L., Kao, H. Y., Chakravarti, D., Lin, R. J., Hassig, C. A., Ayer, D. E., Schreiber, S. L., and Evans, R. M. (1997) Nuclear receptor repression mediated by a complex containing SMRT, mSin3A, and histone deacetylase. *Cell* 89, 373–380.
- Belandia, B., and Parker, M. G. (2003) Nuclear receptors: a rendezvous for chromatin remodeling factors. *Cell* 114, 277–280.
- Robyr, D., Wolffe, A., and Wahli, W. (2000) Nuclear hormone receptor coregulators in action: diversity for shared tasks. *Mol. Endocrinol.* 14, 329–347.
- Zhu, Y., Qi, C., Calandra, C., Rao, M. S., and Reddy, J. K. (1996) Cloning and identification of mouse steroid receptor coactivator-1 (mSRC-1), as a coactivator of peroxisome proliferator-activated receptor gamma. *Gene Expression* 6, 185–195.
- Hong, H., Kohli, K., Trivedi, A., Johnson, D., and Stallcup, M. (1996) GRIP1, a novel mouse protein that serves as a transcriptional coactivator in yeast for the hormone binding domains of steroid receptors. *Proc. Natl. Acad. Sci. U.S.A.* 93, 4948–4952.
- Voegel, J. J., Heine, M. J., Zechel, C., Chambon, P., and Gronemeyer, H. (1996) TIF2, a 160 kDa transcriptional mediator for the ligand-dependent activation function AF-2 of nuclear receptors. *EMBO J.* 15, 3667–3675.
- Yuan, C., Ito, M., Fondell, J., Fu, Z., and Roeder, R. (1998) The TRAP220 component of a thyroid hormone receptor-associated protein (TRAP) coactivator complex interacts directly with nuclear receptors in a ligand-dependent fashion. *Proc. Natl. Acad. Sci. U.S.A.* 95, 7939–7944.
- Rachez, C., Lemon, B., Suldan, Z., Bromleigh, V., Gamble, M., Naar, A., Erdjument-Bromage, H., Tempst, P., and Freedman, L. (1999) Ligand-dependent transcription activation by nuclear receptors requires the DRIP complex. *Nature* 398, 824–828.
- Renaud, J., Rochel, N., Ruff, M., Vivat, V., Chambon, P., Gronemeyer, H., and Moras, D. (1995) Crystal structure of the RAR-gamma ligand-binding domain bound to all-trans retinoic acid. *Nature* 378, 681–689.
- Shiau, A., Barstad, D., Loria, P., Cheng, L., Kushner, P., Agard, D., and Greene, G. (1998) The structural basis of estrogen receptor/coactivator recognition and the antagonism of this interaction by tamoxifen. *Cell* 95, 927–937.
- Kim, S., Shevde, N. K., and Pike, J. W. (2005) 1,25-Dihydroxy-vitamin D3 stimulates cyclic vitamin D receptor/retinoid X receptor DNA-binding, co-activator recruitment, and histone acetylation in intact osteoblasts. *J. Bone Miner. Res.* 20, 305–317.
- Li, Y., Lambert, M. H., and Xu, H. E. (2003) Activation of nuclear receptors: a perspective from structural genomics. *Structure* 11, 741–746.
- Perissi, V., Staszewski, L., McInerney, E., Kurokawa, R., Krones, A., Rose, D., Lambert, M., Milburn, M., Glass, C., and Rosenfeld, M. (1999) Molecular determinants of nuclear receptor-corepressor interaction. *Genes Dev.* 13, 3198–3208.
- Xu, H. E., Stanley, T. B., Montana, V. G., Lambert, M. H., Shearer, B. G., Cobb, J. E., McKee, D. D., Galardi, C. M., Plunket, K. D., Nolte, R. T., Parks, D. J., Moore, J. T., Kliewer, S. A., Willson, T. M., and Stimmel, J. B. (2002) Structural basis for antagonist-mediated recruitment of nuclear co-repressors by PPARalpha. *Nature* 415, 813–817.
- Heery, D., Kalkhoven, E., Hoare, S., and Parker, M. (1997) A signature motif in transcriptional co-activators mediates binding to nuclear receptors. *Nature* 387, 733–736.
- Vanhooke, J. L., Benning, M. M., Bauer, C. B., Pike, J. W., and DeLuca, H. F. (2004) Molecular structure of the rat vitamin D receptor ligand binding domain complexed with 2-carbon-substituted vitamin D3 hormone analogues and a LXXLL-containing coactivator peptide. *Biochemistry* 43, 4101–4110.
- Jurutka, P. W., Hsieh, J. C., Remus, L. S., Whitfield, G. K., Thompson, P. D., Haussler, C. A., Blanco, J. C., Ozato, K., and Haussler, M. R. (1997) Mutations in the 1,25-dihydroxyvitamin D3 receptor identifying C-terminal amino acids required for transcriptional activation that are functionally dissociated from hormone binding, heterodimeric DNA binding, and interaction with basal transcription factor IIB, in vitro. *J. Biol. Chem.* 272, 14592–14599.
- Jimenez-Lara, A. M., and Aranda, A. (1999) Lysine 246 of the vitamin D receptor is crucial for ligand-dependent interaction with coactivators and transcriptional activity. *J. Biol. Chem.* 274, 13503–13510.
- Hu, X., and Lazar, M. (1999) The CoNR motif controls the recruitment of corepressors by nuclear hormone receptors. *Nature* 402, 93–96.
- Nagy, L., Kao, H., Love, J., Li, C., Banayo, E., Gooch, J., Krishna, V., Chatterjee, K., Evans, R., and Schwabe, J. (1999) Mechanism of corepressor binding and release from nuclear hormone receptors. *Genes Dev.* 13, 3209–3216.
- Cachon-Gonzalez, M. B., Fenner, S., Coffin, J. M., Moran, C., Best, S., and Stoye, J. P. (1994) Structure and expression of the hairless gene of mice. *Proc. Natl. Acad. Sci. U.S.A.* 91, 7717–7721.
- Xie, Z., Chang, S., Oda, Y., and Bikle, D. D. (2006) Hairless suppresses vitamin D receptor transactivation in human keratinocytes. *Endocrinology* 147, 314–323.
- Hsieh, J. C., Sisk, J. M., Jurutka, P. W., Haussler, C. A., Slater, S. A., Haussler, M. R., and Thompson, C. C. (2003) Physical and functional interaction between the vitamin D receptor and hairless corepressor, two proteins required for hair cycling. *J. Biol. Chem.* 278, 38665–38674.
- Cichon, S., Anker, M., Vogt, I. R., Rohleder, H., Putzstuck, M., Hillmer, A., Farooq, S. A., Al-Dhafri, K. S., Ahmad, M., Haque, S., Rietschel, M., Propping, P., Kruse, R., and Nothen, M. M.

- (1998) Cloning, genomic organization, alternative transcripts and mutational analysis of the gene responsible for autosomal recessive universal congenital alopecia. *Hum. Mol. Genet.* 7, 1671–1679.
32. Li, Y. C., Pirro, A. E., Amling, M., Dellling, G., Baron, R., Bronson, R., and Demay, M. B. (1997) Targeted ablation of the vitamin D receptor: an animal model of vitamin D-dependent rickets type II with alopecia. *Proc. Natl. Acad. Sci. U.S.A.* 94, 9831–9835.
33. Yoshizawa, T., Handa, Y., Uematsu, Y., Takeda, S., Sekine, K., Yoshihara, Y., Kawakami, T., Arioka, K., Sato, H., Uchiyama, Y., Masushige, S., Fukamizu, A., Matsumoto, T., and Kato, S. (1997) Mice lacking the vitamin D receptor exhibit impaired bone formation, uterine hypoplasia and growth retardation after weaning. *Nat. Genet.* 16, 391–396.
34. Potter, G. B., Zarach, J. M., Sisk, J. M., and Thompson, C. C. (2002) The thyroid hormone-regulated corepressor hairless associates with histone deacetylases in neonatal rat brain. *Mol. Endocrinol.* 16, 2547–2560.
35. Moraitis, A. N., Giguere, V., and Thompson, C. C. (2002) Novel mechanism of nuclear receptor corepressor interaction dictated by activation function 2 helix determinants. *Mol. Cell. Biol.* 22, 6831–6841.
36. Skorija, K., Cox, M., Sisk, J. M., Dowd, D. R., MacDonald, P. N., Thompson, C. C., and Demay, M. B. (2005) Ligand-independent actions of the vitamin D receptor maintain hair follicle homeostasis. *Mol. Endocrinol.* 19, 855–862.
37. Panteleyev, A. A., Botchkareva, N. V., Sundberg, J. P., Christiano, A. M., and Paus, R. (1999) The role of the hairless (hr) gene in the regulation of hair follicle catagen transformation. *Am. J. Pathol.* 155, 159–171.
38. Perakyla, M., Malinen, M., Herzig, K. H., and Carlberg, C. (2005) Gene regulatory potential of nonsteroidal vitamin D receptor ligands. *Mol. Endocrinol.* 19, 2060–2073.
39. Boehm, M. F., Fitzgerald, P., Zou, A., Elgort, M. G., Bischoff, E. D., Mere, L., Mais, D. E., Bissonnette, R. P., Heyman, R. A., Nadzan, A. M., Reichman, M., and Allegretto, E. A. (1999) Novel nonsecosteroidal vitamin D mimics exert VDR-modulating activities with less calcium mobilization than 1,25-dihydroxyvitamin D₃. *Chem. Biol.* 6, 265–275.
40. Moore, J. M., Galicia, S. J., McReynolds, A. C., Nguyen, N. H., Scanlan, T. S., and Guy, R. K. (2004) Quantitative proteomics of the thyroid hormone receptor-coregulator interactions. *J. Biol. Chem.* 279, 27584–27590.
41. Estebanez-Perpina, E., Moore, J. M., Mar, E., Delgado-Rodriguez, E., Nguyen, P., Baxter, J. D., Buehrer, B. M., Webb, P., Fletterick, R. J., and Guy, R. K. (2005) The molecular mechanisms of coactivator utilization in ligand-dependent transactivation by the androgen receptor. *J. Biol. Chem.* 280, 8060–8068.
42. Krylova, I. N., Sablin, E. P., Moore, J., Xu, R. X., Waitt, G. M., MacKay, J. A., Juzumiene, D., Bynum, J. M., Madauss, K., Montana, V., Lebedeva, L., Suzawa, M., Williams, J. D., Williams, S. P., Guy, R. K., Thornton, J. W., Fletterick, R. J., Willson, T. M., and Ingraham, H. A. (2005) Structural analyses reveal phosphatidyl inositols as ligands for the NR5 orphan receptors SF-1 and LRH-1. *Cell* 120, 343–355.
43. Rochel, N., Wurtz, J. M., Mitschler, A., Klaholz, B., and Moras, D. (2000) The crystal structure of the nuclear receptor for vitamin D bound to its natural ligand. *Mol. Cell* 5, 173–179.
44. Zamir, I., Harding, H. P., Atkins, G. B., Horlein, A., Glass, C. K., Rosenfeld, M. G., and Lazar, M. A. (1996) A nuclear hormone receptor corepressor mediates transcriptional silencing by receptors with distinct repression domains. *Mol. Cell. Biol.* 16, 5458–5465.
45. McKenna, N., Lanz, R., and O'Malley, B. (1999) Nuclear receptor coregulators: cellular and molecular biology. *Endocr. Rev.* 20, 321–344.
46. Jurutka, P. W., Hsieh, J. C., Nakajima, S., Haussler, C. A., Whitfield, G. K., and Haussler, M. R. (1996) Human vitamin D receptor phosphorylation by casein kinase II at Ser-208 potentiates transcriptional activation. *Proc. Natl. Acad. Sci. U.S.A.* 93, 3519–3524.
47. Bramlett, K. S., Wu, Y., and Burris, T. P. (2001) Ligands specify coactivator nuclear receptor (NR) box affinity for estrogen receptor subtypes. *Mol. Endocrinol.* 15, 909–922.
48. Liao, L., Kuang, S. Q., Yuan, Y., Gonzalez, S. M., O'Malley, B. W., and Xu, J. (2002) Molecular structure and biological function of the cancer-amplified nuclear receptor coactivator SRC-3/AIB1. *J. Steroid Biochem. Mol. Biol.* 83, 3–14.
49. McInerney, E. M., Rose, D. W., Flynn, S. E., Westin, S., Mullen, T. M., Krones, A., Inostroza, J., Torchia, J., Nolte, R. T., Assa-Munt, N., Milburn, M. V., Glass, C. K., and Rosenfeld, M. G. (1998) Determinants of coactivator LXXLL motif specificity in nuclear receptor transcriptional activation. *Genes Dev.* 12, 3357–3368.
50. Chang, C., Norris, J. D., Gron, H., Paige, L. A., Hamilton, P. T., Kenan, D. J., Fowlkes, D., and McDonnell, D. P. (1999) Dissection of the LXXLL nuclear receptor-coactivator interaction motif using combinatorial peptide libraries: discovery of peptide antagonists of estrogen receptors alpha and beta. *Mol. Cell. Biol.* 19, 8226–8239.
51. Nolte, R. T., Wisely, G. B., Westin, S., Cobb, J. E., Lambert, M. H., Kurokawa, R., Rosenfeld, M. G., Willson, T. M., Glass, C. K., and Milburn, M. V. (1998) Ligand binding and co-activator assembly of the peroxisome proliferator-activated receptor-gamma. *Nature* 395, 137–143.
52. Zella, L. A., Chang, C. Y., McDonnell, D. P., and Wesley Pike, J. (2007) The vitamin D receptor interacts preferentially with DRIP205-like LxxLL motifs. *Arch. Biochem. Biophys.* 460, 206–212.
53. Vanhooke, J. L., Tadi, B. P., Benning, M. M., Plum, L. A., and DeLuca, H. F. (2007) New analogs of 2-methylene-19-nor-(20S)-1,25-dihydroxyvitamin D₃ with conformationally restricted side chains: evaluation of biological activity and structural determination of VDR-bound conformations. *Arch. Biochem. Biophys.* 460, 161–165.
54. Rachez, C., Gamble, M., Chang, C., Atkins, G., Lazar, M., and Freedman, L. (2000) The DRIP complex and SRC-1/p160 co-activators share similar nuclear receptor binding determinants but constitute functionally distinct complexes. *Mol. Cell. Biol.* 20, 2718–2726.
55. Tagami, T., Lutz, W. H., Kumar, R., and Jameson, J. L. (1998) The interaction of the vitamin D receptor with nuclear receptor corepressors and coactivators. *Biochem. Biophys. Res. Commun.* 253, 358–363.
56. Sanchez-Martinez, R., Zambrano, A., Castillo, A. I., and Aranda, A. (2008) Vitamin D-dependent recruitment of corepressors to vitamin D/retinoid X receptor heterodimers. *Mol. Cell. Biol.* 28, 3817–3829.
57. Ciesielski, F., Rochel, N., and Moras, D. (2007) Adaptability of the vitamin D nuclear receptor to the synthetic ligand Gemini: remodelling the LBP with one side chain rotation. *J. Steroid Biochem. Mol. Biol.* 103, 235–242.
58. Shimizu, M., Miyamoto, Y., Takaku, H., Matsuo, M., Nakabayashi, M., Masuno, H., Udagawa, N., Deluca, H. F., Ikura, T., and Ito, N. (2008) 2-Substituted-16-ene-22-thia-1-alpha,25-dihydroxy-26,27-dimethyl-19-norvitamin D(3) analogs: Synthesis, biological evaluation, and crystal structure. *Bioorg. Med. Chem.* (in press).
59. Geistlinger, T. R., and Guy, R. K. (2001) An inhibitor of the interaction of thyroid hormone receptor beta and glucocorticoid interacting protein 1. *J. Am. Chem. Soc.* 123, 1525–1526.

BI801874N